Available online at www.sciencedirect.com
ScienceDirect
Bioorganic Chemistry 35 (2007) 284–293
BIOORGANIC CHEMISTRY
www.elsevier.com/locate/bioorg

Synthesis and characterization of CN-modified protein analogues as potential vibrational contrast agents

Matthew Noestheden [a,b], Qingyan Hu [a], Li-Lin Tay [c], Angela M. Tonary [a], Albert Stolow [a], Roger MacKenzie [d], Jamshid Tanha [d], John Paul Pezacki [a,b,*]

[a] *Steacie Institute for Molecular Sciences, National Research Council of Canada, Ottawa, Canada*
[b] *Department of Chemistry, University of Ottawa, Ottawa, Canada*
[c] *Institute for Microstructural Sciences, National Research Council of Canada, Ottawa, Canada*
[d] *Institute for Biological Sciences, National Research Council of Canada, Ottawa, Canada*

Received 1 November 2006
Available online 21 February 2007

Abstract

A recombinant V_H single-domain antibody recognizing staphylococcal protein A was functionalized on reactive lysine residues with *N*-hydroxysuccimidyl-activated 4-cyanobenzoate. Surface plasmon resonance analysis of antibody-antigen binding revealed that modified and unmodified antibodies bound protein A with similar affinities. Raman imaging of the modified antibodies indicated that the benzonitrile group provides vibrational contrast enhancement in a region of the electromagnetic spectrum that is transparent to cellular materials. Thus, the modified single-domain antibody may be amenable to detecting protein A from samples of the human pathogen *Staphylococcus aureus* using vibronic detection schemes such as Raman and coherent anti-Stokes Raman scattering. The generality of this labeling strategy should make it applicable to modifying an array of proteins with varied structure and function.

Keywords: Raman; CARS; SERS; Single-domain antibody; Protein modification; Orthogonal labeling

* Corresponding author. Fax: +1 613 952 0068.
E-mail address: John.Pezacki@nrc.ca (J.P. Pezacki).

0045-2068/$ - see front matter © 2007 Elsevier Inc. All rights reserved.
doi:10.1016/j.bioorg.2006.12.004

1. Introduction

High resolution imaging has the potential to facilitate the detection of the molecular determinants of a disease before a diseased phenotype is present in a given tissue. Vibronic imaging modalities such as infrared and Raman microscopies provide several advantages over conventional fluorescence-based techniques [1–3]. Most notable is the fact that they can produce chemically selective image contrast while being non-invasive [4–8]. This is accomplished by utilizing the natural spectroscopic (vibrational Raman) signatures of cellular components, which obviates the requirement for external tagging with fluorophores. However, the slow image acquisition times of Raman and low spatial resolution of infrared microscopy limit the utility of conventional vibronic imaging. Surface enhanced Raman scattering (SERS) microscopy is one technique that has been successfully applied to biological imaging to overcome these issues [9–12]. Additionally, coherent anti-Stokes Raman scattering (CARS) microscopy has been used for the rapid acquisition of 2-D and 3-D images at subcellular resolutions in live cells [13–19].

Currently, Raman and CARS microscopy are limited to imaging classes of macromolecules as opposed to specific molecular targets. Increasing the utility of Raman and CARS microscopies would facilitate their use in modern applications of high resolution molecular imaging such as pathogen/disease detection and phenotypic screening. To take advantage of these techniques for high resolution imaging with molecular specificity, contrast agents that recognize specific cellular targets are required. Here we describe a strategy to add molecular specificity to Raman and CARS microscopies by utilizing HVHP428, a recombinant V_H single-domain antibody (sdAb) recognizing protein A. This methodology has potential clinical applications as protein A is a cell surface protein of *Staphylococcus aureus*, a pathogenic human bacterium.

The *N*-hydroxysuccinimide (NHS) bioconjugation reaction was employed to incorporate nitrile (CN) modes onto extant proteins for the purpose of *in vivo* tracking using Raman and CARS microscopies. Nitrile groups were chosen because they possess orthogonal vibrational modes when compared to endogenous cellular materials. Optimization of the protocol was demonstrated using bovine serum albumin (BSA). Furthermore, analysis of a 4-CN-benzoyl-NHS (4-CN-NHS)-modified HVHP428 (HVHP428-CN) was carried out to determine the functional effect of introducing 4-CN-benzyl groups. The methods developed herein should be applicable to other sdAbs and proteins in general.

2. Materials and methods

All chemicals were purchased from Aldrich (Oakville, ON, Canada) and used as received. Eighteen milliohm H_2O was obtained from a NANOpure® Diamonds™ Life Science Series 1370 water filtration system (Barnstead International, Dubuque, IO, USA).

2.1. Synthesis of 4-CN-NHS

4-Cyano-benzoyl chloride (63 mg, 0.38 mmol) was suspended in 2 mL dichloromethane. NHS (48 mg, 0.42 mmol) and 50 μL triethylamine in 2 mL dichloromethane were added under argon. The mixture was stirred for 1 h at room temperature and then extracted with 0.1 M NaOH (5 mL × 3). The organic layer was concentrated and purified by silica

column chromatography (eluted with 1:1 of ethylacetate: hexane) to give 4-CN-NHS (76 mg, 89%). ^{1}H NMR (400 MHz, $CDCl_3$) 8.28 (d, 2H), 7.86 (d, 2H), 2.97 (s, 4H).

2.2. Expression and purification of sdAbs

For a complete review pertaining to the generation of sdAbs see [20,21]. Expression and purification of the recombinant sdAb was carried out as outlined in [22], except periplasmic extraction was performed instead of cell lysis. Briefly, harvested *Escherichia coli* containing the expressed sdAbs were washed once with 10 mM Tris, pH 8.0, after which a 10 min incubation at room temperature in sucrose solution (25% sucrose, 1 mM EDTA, 10 mM Tris, pH 8.0) was performed. Following centrifugation, the resulting pellet was resuspended in ice cold shock solution (10 mM Tris, pH 8.0, 0.5 mM $MgCl_2$) for 5–10 min on ice. After centrifugation the retentates were further purified as outlined in [22].

2.3. Protein labeling

Labeling of BSA and HVHP428 was accomplished by mixing solutions of ca. 5 mg/mL of protein (100 mM $NaHCO_3$, pH 8.3) with an equal volume of 25 mM 4-CN-NHS in DMSO. Successful labelling was achieved with protein concentrations ranging from 0.3 to 5 mg/mL. The labeling reaction was allowed to proceed for 1 h at 37 °C. After a 1:10 dilution with H_2O, the labeled protein was purified by passage through a YM10 MWCO filter and further cleaned via two H_2O washes. The retentate was collected and characterized using MALDI, as well as Raman spectroscopy and microscopy.

2.4. MALDI analysis

For MALDI analysis, protein samples were desalted on a C4 ZipTip (Millipore) and eluted with 70% (v/v) aqueous acetonitrile containing 0.1% (v/v) trifluoroacetic acid (TFA). The desalted sample (1 μL) was spotted on a target plate with an equal volume of sinapinic acid solution [12 mg/mL in aqueous solution with 0.1% (v/v) TFA and 33% (v/v) acetonitrile] and dried. The plate was analyzed on a Voyager DE-Pro MALDI-ToF (Applied Biosystem, Foster City, CA, USA) mass spectrometer operated in the linear/positive-ion mode. Instrument configuration was as follows: Accelerating voltage, 25,000; Grid Voltage, 92%; Guide Wire Voltage, 0.010%; Delay Time, 380 ns; Low Mass Gate, 2000 Da; LaserPower, 2174; and Shots/spectrum, 200.

2.5. Raman microscopy and spectroscopy

Raman samples were prepared by spotting 0.5 μL of each protein onto a phosphorous-doped N-type silicon substrate (single-side polished, 250 ± 25 μm thickness; Virginia Semiconductor Incorporated, Fredericksburg, VA, USA) and drying at ambient temperature. Raman spectroscopy and microscopy were carried out using a confocal Raman microscope (Horiba Jobin Yvon, Edison, NJ, USA) configured in a back scattering geometry, which was coupled to an Olympus BX51 microscope (Olympus America Incorporated, Center Valley, PA, USA). Scattered light was collected through a high numerical aperture ($N_a = 0.90$) 100× objective (Olympus America Incorporated) and was detected on a 1024×256 element thermo-electrical cooled CCD detector (Andor Technology,

South Windsor, CT, USA). Sample excitation was achieved via a HeNe laser ($\lambda = 632.8$ nm) sharply focused to a diffraction-limited spot, with a focal power density of approximately 10^5 W/cm^2. Typically, spectra were acquired with three accumulations of 20 s. All spectral processing was performed within the manufacturer's instrumental control software, LabSpec 5.14 (Horiba Jobin Yvon). Spectral smoothing was achieved using the Savitsky–Golay smoothing routine. Baseline removal was accomplished by subtracting the raw data to a polynomial-fitted baseline function.

2.6. SPR analysis of modified sdAb

Dissociation constants for modified and unmodified sdAb were determined by surface plasmon resonance (SPR) using the BIACORE 3000 biosensor system (Biacore, Incorporated, Piscataway, NJ, USA). Four hundred resonance units of protein A (Amersham, Buckinghamshire, UK) and 780 resonance units of an unrelated F_{ab} as a reference protein were immobilized on research grade CM5 sensorchip (BIACORE). Immobilizations were carried out at protein concentrations of 25–50 μg/ml in 10 mM acetate buffer, pH 4.5, using the amine coupling kit supplied by the manufacturer. All measurements were carried out at 25 °C in 10 mM Hepes, pH 7.4, containing 150 mM NaCl, 3 mM EDTA and 0.005% P20 at a flow rate of 40 μl/min. No surface regeneration was required. Data was evaluated using BIAevaluation 4.1 (Biacore, Incorporated) and GraphPad Prism software (v 4.01; GraphPad Software, San Diego, CA, USA).

3. Results

3.1. BSA modification

Modification of BSA was performed as described in Section 2 (Fig. 1a). MALDI analysis of normal and 4-CN-NHS-modified BSA (BSA-CN) revealed a mass difference of 901 Da (Fig. 1b), which corresponds to the addition of seven 4-CN-NHS (130 Da/label). Raman microscopy analysis of BSA-CN was carried out as described in Section 2. BSA-CN was spotted onto the silicon substrate and the Raman spectrum of the sample was acquired. A band at 2230 cm^{-1} clearly indicated the presence of the cyano group in the protein sample. To further confirm that the 2230 cm^{-1} band was from BSA-CN and not residual 4-CN-NHS reagent, two false colored intensity maps were generated by scanning the protein spot, collecting Raman spectra for each pixel, and integrating for the CN Raman band at 2230 cm^{-1} and amide I band at 1650 cm^{-1}, respectively (Fig. 2). The two maps showed clear spatial co-localization of the CN vibrational mode and amide I band. These findings provided strong evidence that the labeling reaction was successful.

3.2. Single-domain antibody modification

Modification of HVHP428 was performed as described in Section 2. MALDI analysis of 4-CN-NHS modified (HVHP428-CN) and unmodified HVHP428 revealed a mass difference of 248 Da (Fig. 3). Assuming an error of ±10 Da on the experimentally determined molecular weight, the MALDI data indicated that approximately two 4-CN-NHS groups were conjugated to the antibody. Further confirmation of the labeling success was obtained via Raman spectroscopy, which showed a clear CN band at around 2230 cm^{-1}

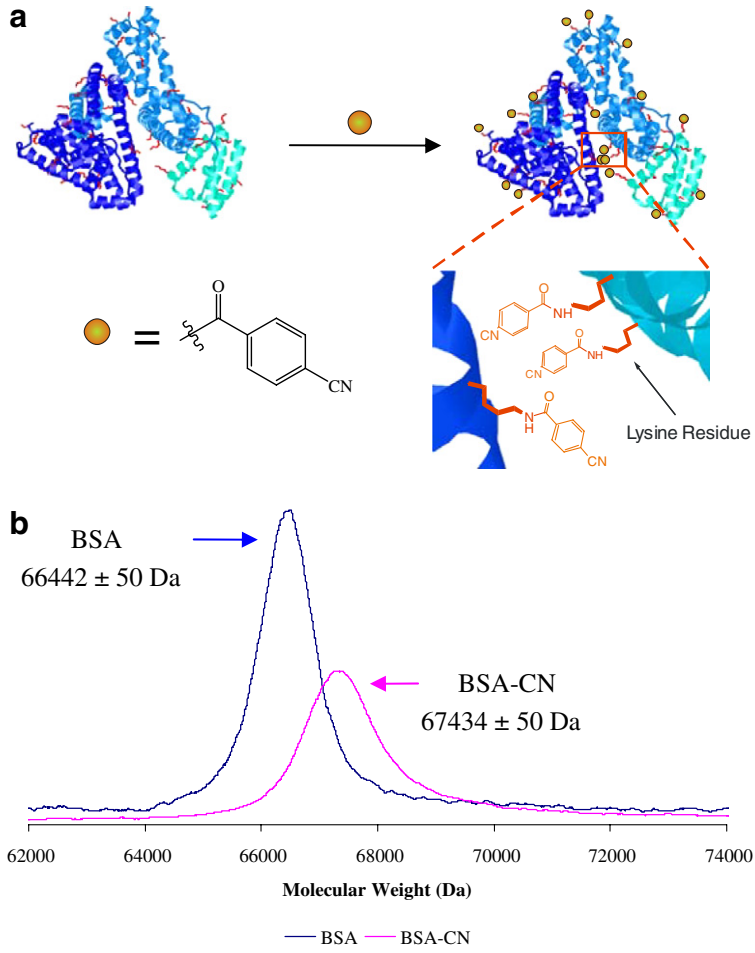

Fig. 1. Protein modification using NHS-activated acids. (a) Schematic representation of the approach used to modify BSA. Lysine residues are highlighted in red. The positions of the CN labels on BSA-CN are not indicative of the actual residues modified, but rather are shown for illustrative purposes; (b) MALDI revealed a mass difference of approximately 900 Da, which corresponds to the incorporation of approximately seven 4-CN-NHS vibrational contrast agents per protein. (For interpretation of the references to color in this figure legend, the reader is referred to the web version of this paper.)

when HVHP428-CN was analyzed (Fig. 4). The limited number of CN modes per molecule of HVHP428 yielded a poor signal-to-noise ratio that was not suitable for generating image contrast using Raman microscopy (data not shown). This may be sufficient for SERS or CARS microscopy, however.

3.3. Functional validation of HVHP428-CN

To establish the functional effect of modifying HVHP428 with 4-CN-NHS, SPR analysis of the interaction between HVHP428-CN and protein A was measured using Biacore analysis as described in Section 2. Comparison of the dissociation constants (K_d) for

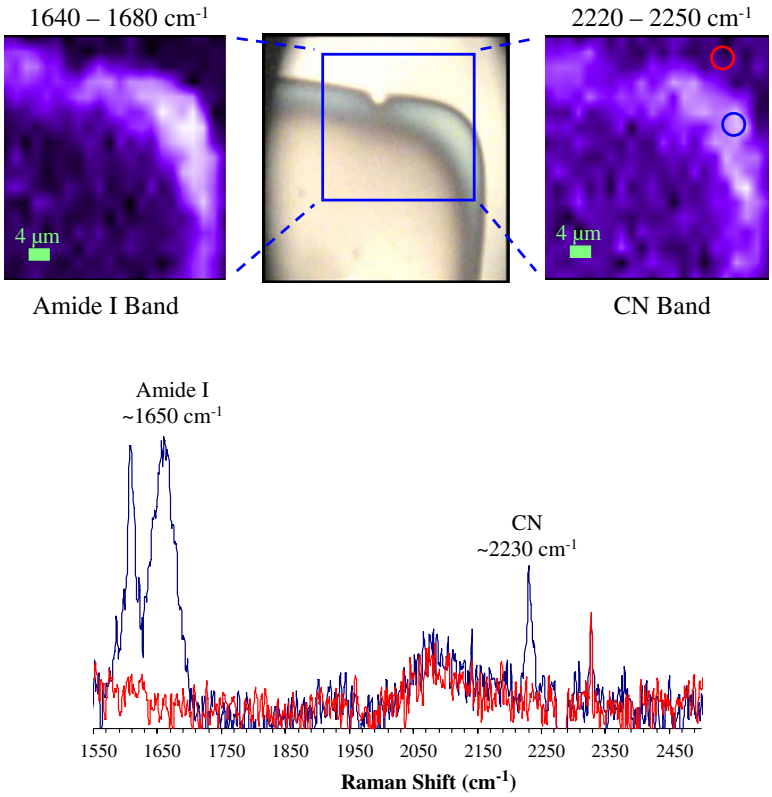

Fig. 2. Raman microscopic and spectroscopic analyses of BSA-CN. Top right image depicts the intensity distribution of the CN vibrational band (~2230 cm^{-1}), which was generated by integrating the area under the CN band. The bright areas indicate regions with strong CN band intensity, while the dark purple areas correspond to regions of minimal/no CN band intensity. Integration of the amide I band (top left; approximately 1650 cm^{-1}) yielded an intensity image that was spatially co-localized with the CN intensity map. This strong spatial correlation between the CN and amide I modes suggested that modification was successful and specific to the protein rather than to residual 4-CN-NHS. The blue spectrum taken from an intense region (blue circle) of the imaged area showed both amide I and CN vibrational modes. The red spectrum taken from a region of the map corresponding to bare silicon substrate (red circle) was devoid of any analyte-specific vibrational bands. The blue rectangle in the optical image (top center) shows the region that was imaged. (For interpretation of the references to color in this figure legend, the reader is referred to the web version of this paper.)

unmodified (1.5 ± 0.1 μM) and modified (1.7 ± 0.2 μM) HVHP428 revealed that 4-CN-NHS modification had no appreciable effect on the ability of the HVHP428 to recognize its antigenic target (Fig. 5).

4. Discussion

Vibronic contrast agents are becoming important tools for molecular imaging. In order to develop such agents containing CN modes we first labeled BSA, which is an approximately 66 kDa soluble protein that has been used extensively as a model system in the development of protein labeling strategies. In particular, due to the presence of 60 lysine

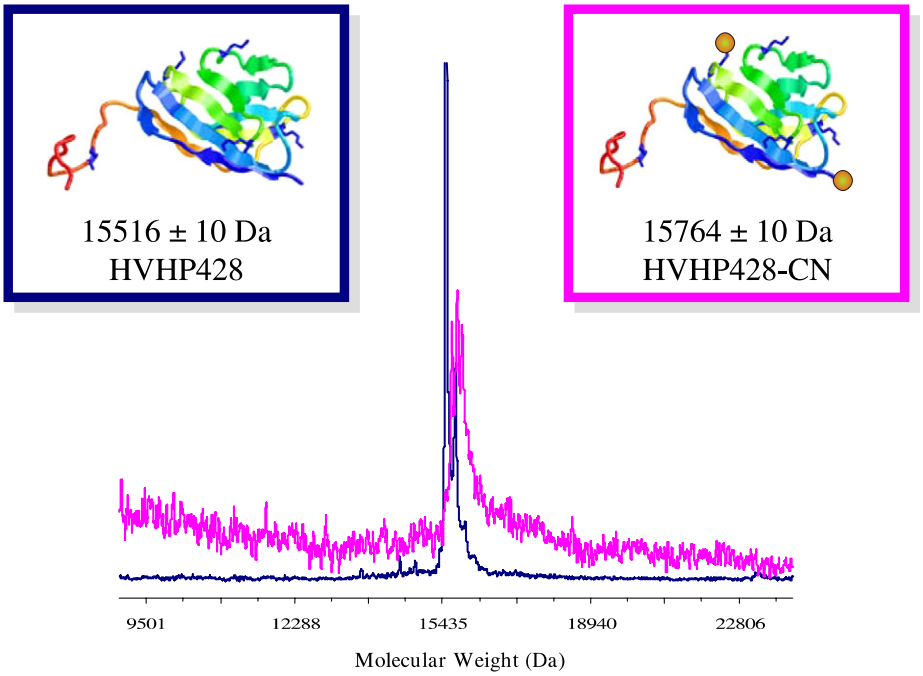

Fig. 3. MALDI analysis of HVHP428-CN. The mass difference of 248 Da between unmodified (blue) and modified (pink) HVHP428 correlated to approximately two 4-CN-modified lysine residues per protein. Protein structures and sites of modification are shown for illustrative purposes and do not represent HVHP428. (For interpretation of the references to color in this figure legend, the reader is referred to the web version of this paper.)

residues (~10% of the primary sequence), BSA has been successfully applied to the development of amine-directed labeling using NHS- and isothiocyanate-functionalized small molecules [23–30]. MALDI analysis of BSA-CN showed an increased mass for the labeled protein that corresponded to the modification of seven residues with 4-CN-NHS (Fig. 1b). Assuming that labeling occurred only on lysine residues, this correlates to a labeling efficiency of approximately 10%. While seemingly low, this value was likely skewed because only the exposed lysines will react efficiently with our probe molecule. The Raman analysis of BSA-CN displayed a clear CN mode in the observed spectrum that was spatially localized with the protein amide I band at approximately 1650 cm^{-1} (Fig. 2). This showed that BSA could be functionalized with CN modes and that vibrational contrast specific to BSA-CN could be generated. Furthermore, these results gave a strong indication that tissue or cellular Raman imaging of CN-modified proteins may be possible.

The prevalence of chemically modified antibodies that are utilized for indirect immunofluorescence demonstrates that modified proteins can maintain their efficacy following functionalization. Conversely, chemical elaboration has also been shown to affect the physicochemical properties of modified proteins and alter their *in vivo* function [31,32]. These antithetic findings suggest that a labeling methodology that was effective for BSA would not necessarily be predictive of successfully modifying other proteins. However, the application of protocols established on BSA and subsequently used to modify other

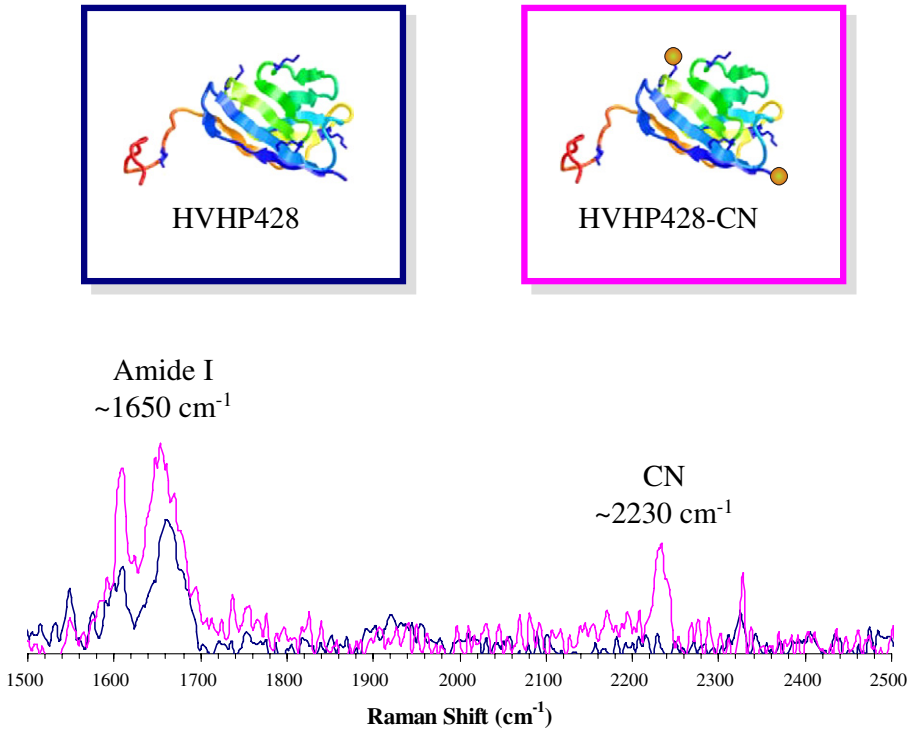

Fig. 4. Raman spectra of HVHP428-CN. Spectroscopic analysis revealed the presence of the amide I band ($\sim$1650 cm^{-1}) in both spectra, which confirmed that it was protein being examined. Further analysis showed that HVHP428-CN (pink) clearly displayed a CN band ($\sim$2230 cm^{-1}) that was absent for HVHP428 (blue). (For interpretation of the references to color in this figure legend, the reader is referred to the web version of this paper.)

proteins illustrates the validity of this approach [23–30]. Therefore, a model system with a well-defined and easily assayed function was needed to determine the functional consequences of 4-CN modification using the protocol established for BSA.

Antibody-antigen recognition was an excellent candidate to assay for the effects of 4-CN-NHS modification because antigen recognition is closely linked to antibody structure. However, using mono- and polyclonal antibodies is difficult because the analysis of functional labeling is complicated by several factors: (1) the size (approximately 160 kDa) would limit the quantification of the number of CN modes by MALDI; and (2) the presence of disulfide linkages and the complex secondary and tertiary interactions that define antibody function may all be modulated to varying degrees by the presence of CN modifications. On the other hand, a structurally simplistic and smaller ($\sim$14 kDa) family of proteins known as single-domain antibodies provided a bio-recognition system that was better suited to the analytical methods employed in the current study to characterize CN-modification and also serve as stable reagents for vibronic contrast. Furthermore, the functional consequences of 4-CN-NHS modification of sdAbs could be easily assayed by quantifying antibody-antigen binding.

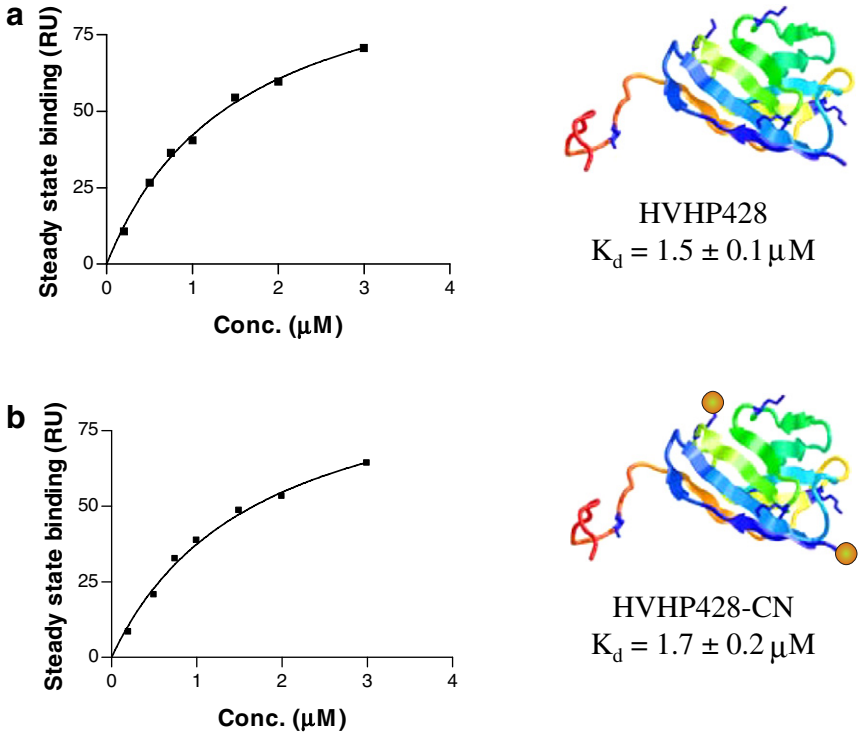

Fig. 5. Functional validation of HVHP428-CN. (a) Analysis of HVHP428 showed that it bound protein A with a $K_d = 1.5 \pm 0.2$ μM. (b) Similar analysis of HVHP428-CN revealed no appreciable difference in protein A binding, with $K_d = 1.7 \pm 0.2$ μM. Crystal structures and sites of modification are shown for illustrative purposes and do not represent HVHP428.

MALDI analysis of HVHP428 following reaction with 4-CN-NHS revealed that two CN modes were incorporated per protein (Fig. 3) and Raman spectral analysis of HVHP428-CN revealed the clear presence of the CN mode (Fig. 4). The combination of MALDI and Raman spectral data gave definitive evidence that the generation of HVHP428-CN was successful. Subsequent attempts to confirm this result using Raman microscopy were hindered due to the low number of CN modes per HVHP428 (data not shown). As such, it would be advantageous to establish methods of increasing the labeling efficiency of the 4-CN-NHS reaction. Augmenting the concentration of 4-CN-NHS and the incubation time of the labeling reaction is currently being pursued to address this problem.

SPR analysis was performed to determine the functional effects of HVHP428 modification with 4-CN-NHS. Analysis revealed that the K_d of HVHP428 for protein A was 1.5 ± 0.1 μM and that of HVHP428-CN was 1.7 ± 0.2 μM (Fig. 5). This indicates that the functional consequences of incorporating 4-CN-NHS were negligible. This also shows that the modified residues did not play an integral role in the structure and/or function of HVHP428.

Herein we show that larger proteins capable of accommodating more modifications (BSA) are able to generate Raman image contrast that is specific to the CN mode contained on labeled proteins. In addition, the modification of HVHP428 with 4-CN-NHS

appeared to have no effect on the wild-type function of the antibody. These CN-labeled sdAb conjugates have potential applications to live cell imaging using Raman or CARS microscopy. They also may serve as novel immunochemical recognition elements if used to coat SERS-active substrates. These exciting avenues are currently under investigation.

Acknowledgments

We thank Y. Rouleau, S. Belanger, and S. Ryan for their assistance in preparing and purifying protein samples and T. Hirama for help with binding experiments. We thank the Canadian Institutes for Health Research (CIHR) for financial support of this work.

References

[1] M. Valko, C.J. Rhodes, J. Moncol, M. Izakovic, M. Mazur, Chem. Biol. Interact. 160 (2006) 1–40.
[2] Y. Cakir, S.W. Ballinger, Antiox. Redox Signal. 7 (2005) 726–740.
[3] A. Terman, U.T. Brunk, Antiox. Redox Signal. 8 (2006) 197–204.
[4] W.E. Huang, R.I. Griffiths, I.P. Thompson, M.J. Bailey, A.S. Whiteley, Anal. Chem. 76 (2004) 4452–4458.
[5] Y.-S. Huang, T. Karashima, M. Yamamoto, H. Hamaguchi, Biochemistry 44 (2005) 10009–10019.
[6] J.R. Mourant, K.W. Short, S. Carpenter, N. Kunapareddy, L. Coburn, T.M. Powers, J.P. Freyer, J. Biomed. Opt. 10 (2005) 031106.
[7] K.C. Schuster, I. Reese, E. Urlaub, J.R. Gapes, B. Lendl, Anal. Chem. 72 (2000) 5529–5534.
[8] H.J. van Manen, Y.M. Kraan, D. Roos, C. Otto, Proc. Natl. Acad. Sci. USA 102 (2005) 10159–10164.
[9] I. Chourpa, H. Morjani, J.-F. Riou, M. Manfait, FEBS Lett. 397 (1996) 61–64.
[10] C.E. Talley, L. Jusinski, C.W. Hollars, S.M. Lane, T. Huser, Anal. Chem. 76 (2004) 7064–7068.
[11] J. Kneipp, H. Kneipp, W.L. Rice, K. Kneipp, Anal. Chem. 77 (2005) 2381–2385.
[12] K. Kneipp, A.S. Haka, H. Kneipp, K. Adizadegan, N. Yoshizawa, C. Boone, K.E. Shafer-Peltier, J.T. Motz, R.R. Dasari, M.S. Feld, Appl. Spectrosc. 56 (2002) 150.
[13] C.L. Evans, E.O. Potma, M. Puoris'haag, D. Cote, C.P. Lin, X.S. Xie, Proc. Natl. Acad. Sci. USA 102 (2005) 16807–16812.
[14] A.P. Kennedy, J. Sutcliffe, J.-X. Cheng, Langmuir 21 (2005) 6478–6486.
[15] B. Rakic, S.M. Sagan, M. Noestheden, S. Belanger, X. Nan, C.L. Evans, X.S. Xie, J.P. Pezacki, Chem. Biol. 13 (2006) 23–30.
[16] J.-X. Cheng, Y.K. Jia, G. Zheng, X.S. Xie, Biophys. J. 83 (2002) 502–509.
[17] X. Nan, J.-X. Cheng, X.S. Xie, J. Lipid Res. 44 (2003) 2202–2208.
[18] X. Nan, E.O. Potma, X.S. Xie, Biophys. J. 91 (2006) 728–735.
[19] X. Nan, A. Tonary, M.A. Stolow, X.S. Xie, J.P. Pezacki, ChemBioChem. 7 (2006) 1895–1897.
[20] M. Arbabi-Ghahroudi, J. Tanha, R. MacKenzie, Methods Mol. Biol. (2006) in press.
[21] R. To, T. Hirama, M. Arbabi-Ghahroudi, R. MacKenzie, P. Wang, P. Xu, F. Ni, J. Tanha, J. Biol. Chem. 280 (2005) 41395–41403.
[22] J. Zhang, Q. Li, T.-D. Nguyen, T.-L. Tremblay, E. Stone, R. To, J. Kelly, C. Roger MacKenzie, J. Mol. Biol. 341 (2004) 161–169.
[23] K.J. Schafer-Hales, K.D. Belfield, S. Yao, P.K. Frederiksen, J.M. Hales, P.E. Kolattukudy, J. Biomed. Opt. 10 (2005) 051402.
[24] E.P. de Jong, C.A. Lucy, The Analyst 131 (2006) 664–669.
[25] M. Salmain, A. Gorfti, G. Jaouen, Eur. J. Biochem. 258 (1998) 192–199.
[26] H. Akhavan-Tafti, R. DeSilva, K. Sugioka, R.S. Handley, A.P. Schaap, Luminescence 16 (2001) 187–191.
[27] B.K. Hoefelschweiger, A. Duerkop, O.S. Wolfbeis, Anal. Biochem. 344 (2005) 122–129.
[28] D. Osella, P. Pollone, M. Ravera, M. Salmain, G. Jaouen, Bioconjugate Chem. 10 (1999) 607–612.
[29] J. Bautista, M.D. Mateos-Nevado, Biosci. Biotech. Bioch. 62 (1998) 419–423.
[30] N. Weibel, L.J. Charbonniere, M. Guardigli, A. Roda, R. Ziessel, J. Am. Chem. Soc. 126 (2004) 4888–4896.
[31] R.E. Rumbaut, N.R. Harris, A.J. Sial, V.H. Huxley, D.N. Granger, Am. J. Physiol. Heart Circ. Physiol. 276 (1999) H333–H339.
[32] S. Bingaman, V.H. Huxley, R.E. Rumbaut, Microcirculation 10 (2003) 221–231.